1438

Chem. Pharm. Bull. **56**(10) 1438—1444 (2008)

Vol. 56, No. 10

Bioactive Constituents from Chinese Natural Medicines. XXXII.[1)]
Aminopeptidase N and Aldose Reductase Inhibitors from *Sinocrassula indica*: Structures of Sinocrassosides B_4, B_5, C_1, and D_1—D_3

Toshio Morikawa,[a,b] Haihui Xie,[a] Tao Wang,[a] Hisashi Matsuda,[a] and Masayuki Yoshikawa*,[a]

[a] *Kyoto Pharmaceutical University; Misasagi, Yamashina-ku, Kyoto 607–8412, Japan: and* [b] *Pharmaceutical Research and Technology Institute, Kinki University; 3–4–1 Kowakae, Higashi-osaka, Osaka 577–8502, Japan.*

From the methanolic extract of the whole plant of *Sinocrassula indica* (Crassulaceae), six new flavonol glycosides, sinocrassosides B_4 (**1**), B_5 (**2**), C_1 (**3**), D_1 (**4**), D_2 (**5**), and D_3 (**6**), were isolated together with 30 compounds. The structures of **1**—**6** were elucidated on the basis of chemical and physicochemical evidence. In addition, several constituents were found to show inhibitory effects on aminopeptidase N and aldose reductase.

Key words *Sinocrassula indica*; sinocrassoside; aminopeptidase N inhibitor; aldose reductase inhibitor; Crassulaceae

During the course of our studies on bioactive constituents from Chinese natural medicines,[1—17)] we found that the methanolic extract of the whole plant of *Sinocrassula indica* (Crassulaceae) inhibited the increase of serum glucose levels in both sucrose- and glucose-loaded rats.[2)] From the methanolic extract, 15 acylated flavonol glycosides, sinocrassosides A_1—A_{12} and B_1—B_3 (**7**—**21**), were isolated together with 11 flavonoids (**22**—**32**), 2 megastigmanes (**33**, **34**), L-phenylalanine, and guanosine[1—3)] and several fravonoid constituents were found to show hepatoprotective effects on D-galactosamine-induced cytotoxicity in primary cultured mouse hepatocytes.[1)] As a continuing study on the constituents from *S. indica*, we additionally isolated six new flavonol glycosides, sinocrassosides B_4 (**1**), B_5 (**2**), C_1 (**3**), D_1 (**4**), D_2 (**5**), and D_3 (**6**). This paper deals with the isolation and structure elucidation of **1**—**6** as well as aminopeptidase N and aldose reductase inhibitory activities of the isolated compounds.

The methanolic extract from the dried whole plant of *S. indica* (7.7% from the dried plant) was partitioned into an EtOAc–H_2O (1:1, v/v) mixture to furnish an EtOAc-soluble fraction (2.5%) and an aqueous phase. The aqueous phase was further extracted with *n*-BuOH to give an *n*-BuOH-soluble fraction (1.7%) and an H_2O-soluble fraction (3.4%), which was described previously.[2)] From the EtOAc- and *n*-BuOH-soluble fractions, **1** (0.0068%), **2** (0.0007%), **3** (0.0027%), **4** (0.0006%), **5** (0.0074%), and **6** (0.0010%),

were purified using normal- and reversed-phase silica gel chromatographies and finally HPLC.

Structures of Sinocrassosides B_4 (1), B_5 (2), C_1 (3), D_1 (4), D_2 (5), and D_3 (6) Sinocrassoside B_4 (**1**) was isolated as a yellow powder with negative optical rotation ($[\alpha]_D^{25}$ −47.8° in MeOH). In the UV spectrum of **1**, absorption maxima were observed at 257 (log ε 4.49) and 358 (4.37) nm. The IR spectrum of **1** showed absorption bands at 1725, 1655, and 1599 cm^{-1} assignable to ester carbonyl and γ-pyrone functions and aromatic ring and strong absorption bands at 3432 and 1076 cm^{-1} suggestive of a glycoside moiety. The positive- and negative-ion FAB-MS of **1** showed quasimolecular ion peaks at *m/z* 879 (M+Na)$^+$ and *m/z* 855 (M−H)$^-$, respectively. The molecular formula, $C_{38}H_{48}O_{22}$, of **1** was determined by high resolution FAB-MS measurement. Alkaline hydrolysis of **1** with 10% aqueous potassium hydroxide (KOH)–50% aqueous 1,4-dioxane (1:1, v/v) furnished desacyl-sinocrassoside B_4 (**1a**) together with *S*-(+)-2-methylbutyric acid, which was identified by HPLC analysis using an optical rotation detector.[1—3)] Acid hydrolysis of **1a** with 1.0 M HCl liberated quercetin (**28**), together with L-rhamnose and D-glucose, which were identified by HPLC analysis.[1—7,9—13)] The ^{1}H- (DMSO-d_6, Table 1) and ^{13}C-NMR (Table 2) spectra **1a**, which were assigned by various NMR experiments, showed signals assignable to *meta*-coupled aromatic protons [δ 6.47, 6.83 (1H each, both d, *J*=1.8 Hz, 6, 8-H)] and *ortho*- and *meta*-coupled ABC-type protons [δ 6.85 (1H, d,
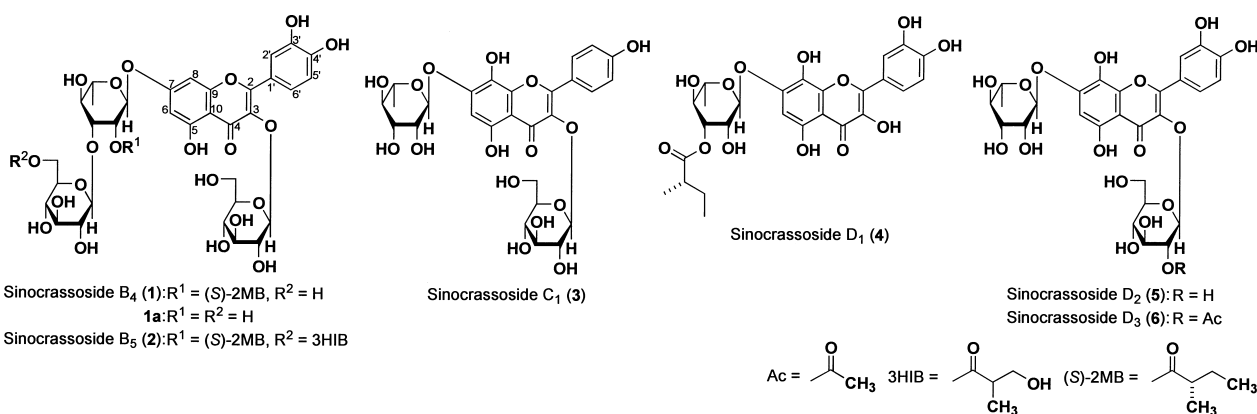

Sinocrassoside B_4 (**1**): R^1 = (S)-2MB, R^2 = H
1a: R^1 = R^2 = H
Sinocrassoside B_5 (**2**): R^1 = (S)-2MB, R^2 = 3HIB

Sinocrassoside C_1 (**3**)

Sinocrassoside D_1 (**4**)

Sinocrassoside D_2 (**5**): R = H
Sinocrassoside D_3 (**6**): R = Ac

Ac = [structure] 3HIB = [structure] (S)-2MB = [structure]

Chart 1

Sinocrassoside A$_1$ (**7**): R = IB
Sinocrassoside A$_2$ (**8**): R = (*S*)-2MB

	R^1	R^2	R^3
Sinocrassoside A$_3$ (**9**):	Ac	H	H
Sinocrassoside A$_4$ (**10**):	H	H	IB
Sinocrassoside A$_5$ (**11**):	Ac	IB	H
Sinocrassoside A$_6$ (**12**):	Ac	(*S*)-2MB	H
Sinocrassoside A$_7$ (**13**):	Ac	H	(*S*)-2MB
Sinocrassoside A$_8$ (**14**):	H	IB	Glc
Sinocrassoside A$_9$ (**15**):	H	(*S*)-2MB	Glc

	R^1	R^2
Sinocrassoside A$_{10}$ (**16**):	H	IB
Sinocrassoside A$_{11}$ (**17**):	Glc	IB
Sinocrassoside A$_{12}$ (**18**):	Glc	3HIB

Sinocrassoside B$_1$ (**19**): R = IB
Sinocrassoside B$_2$ (**20**): R = (*S*)-2MB

Sinocrassoside B$_3$ (**21**)

	R^1	R^2
Kaempferol (**22**):	H	H
Kaempferol 3-*O*-β-D-glucopyranoside (**23**):	Glc	H
Kaempferol 7-*O*-α-L-rhamnopyranoside (**24**):	H	Rha
Kaempferol 3-*O*-β-D-glucopyranosyl-7-*O*-α-L-rhamnopyranoside (**25**):	Glc	Rha
Multiflorin B (**26**):	Rha$\overset{4\ \ 1}{-}$Glc	H
(**27**):	Rha$\overset{4\ \ 1}{-}$Glc	Rha

	R^1	R^2
Quercetin (**28**):	H	H
Quercetin 3-*O*-β-D-glucopyranoside (**29**):	Glc	H
Quercetin 3-*O*-β-D-glucopyranosyl-7-*O*-α-L-rhamnopyranoside (**30**):	Glc	Rha
Multinoside A (**31**):	Rha$\overset{4\ \ 1}{-}$Glc	H

Luteolin (**32**)

trans-(3*S*,5*R*,6*R*,9*S*)-Megastigman-7-ene-3,5,6,9-tetraol 3-*O*-β-D-glucopyranoside (**33**): R^1 = Glc, R^2 = H
trans-(3*S*,5*R*,6*R*,9*S*)-Megastigman-7-ene-3,5,6,9-tetraol 9-*O*-β-D-glucopyranoside (**34**): R^1 = H, R^2 = Glc

Herbacetin (**35**): R^1 = R^2 = H
Gossypetin 7-*O*-α-L-rhamnopyranoside (**36**): R^1 = Rha, R^2 = OH
Gossypetin (**37**): R^1 = H, R^2 = OH

IB = [structure]
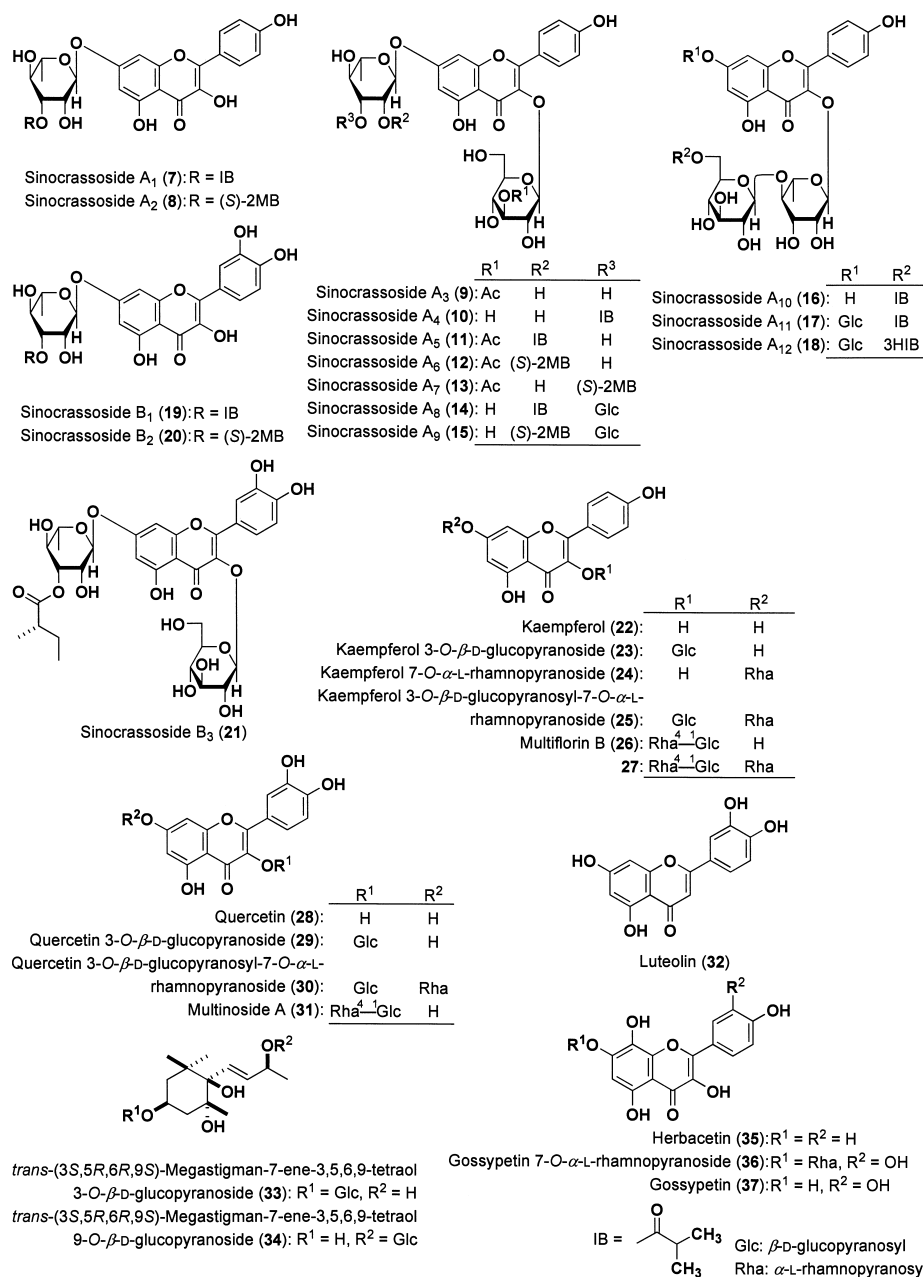Glc: β-D-glucopyranosyl
Rha: α-L-rhamnopyranosyl

Chart 2

J=8.2 Hz, 5′-H), 7.62 (1H, dd, J=2.1, 8.2 Hz, 6′-H), 7.63 (1H, d, J=2.1 Hz, 2′-H)] together with two β-D-glucopyranosyl and a α-L-rhamnopyranosyl moieties [δ 1.14 (3H, d, J=5.6 Hz, Rha-6-H$_3$), 4.48 (1H, d, J=7.6 Hz, 7-*O*-terminal-Glc-1-H), 5.49 (1H, d, J=7.3 Hz, 3-*O*-Glc-1-H), 5.59 (1H, br s, Rha-1-H)]. The connectivities of glycopyranosyl parts were determined by a heteronuclear multiple-bond correlations (HMBC) experiment on **1a**. Namely, long-range correlations were observed between the following protons and carbons [3-*O*-Glc-1-H and 3-C (δ$_C$ 133.5), Rha-1-H and 7-C (δ$_C$ 161.2), and 7-*O*-terminal-Glc-1-H and Rha-3-C (δ$_C$ 80.6)]. Consequently, the structure of **1a** was determined as quercetin 3-*O*-β-D-glucopyranosyl-7-*O*-β-D-glucopyranosyl-(1→3)-α-L-rhamnopyranoside. The ^{1}H- (DMSO-d_6, Table 1) and ^{13}C-NMR (Table 2) spectra of **1** showed signals assignable to a desacyl-sinocrassoside B$_4$ part {a quercetin part [δ

6.52, 6.89 (1H each, both d, J=1.8 Hz, 6, 8-H), 6.86 (1H, d, J=8.2 Hz, 5′-H), 7.62 (1H, dd, J=2.1, 8.2 Hz, 6′-H), 7.63 (1H, d, J=2.1 Hz, 2′-H)] and two β-D-glucopyranosyl and a α-L-rhamnopyranosyl moieties [δ 1.18 (3H, d, J=5.8 Hz, Rha-6-H$_3$), 4.47 (1H, d, J=7.6 Hz, 7-*O*-terminal-Glc-1-H), 5.49 (1H, d, J=7.0 Hz, 3-*O*-Glc-1-H), 5.70 (1H, br s, Rha-1-H)]} together with (2*S*)-2-methylbutyryl moiety [δ 0.93 (3H, dd, J=7.4, 7.4 Hz, 2MB-4-H$_3$), 1.12 (3H, d, J=7.0 Hz, 2MB-5-H$_3$), 1.50, 1.64 (1H each, both ddq, J=7.0, 14.0, 7.4 Hz, 2MB-3-H$_2$), 2.45 (1H, ddq, J=7.0, 7.0, 7.0 Hz, 2MB-2-H)]. In the HMBC experiment of **1**, a long-range correlation was observed between the Rha-2-proton [δ 5.36 (1H, br s)] and the (2*S*)-2-methylbutyryl ester carbonyl carbon (δ$_C$ 175.3), so that the structure of sinocrassoside B$_4$ was elucidated as quercetin 3-*O*-β-D-glucopyranosyl-7-*O*-β-D-glucopyranosyl-(1→3)-α-L-[2-*O*-(2*S*)-2-methylbutyryl]-rhamnopyranoside

(1).

Sinocrassoside B$_5$ (**2**), C$_{42}$H$_{54}$O$_{24}$, was also observed as a yellow powder with negative optical rotation ([α]$_D^{25}$ −64.5° in MeOH). Alkaline hydrolysis of **2** with 10% KOH–50% aqueous 1,4-dioxane (1:1, v/v) furnished **1a** together with (S)-(+)-2-methylbutyric acid and 3-hydroxyisobutyric acid, which were identified by HPLC analysis of their p-nitrobenzyl derivatives[1—4,6,7,12] and/or using an optical rotation detector. The proton and carbon signals in the ^{1}H- (DMSO-d_6, Table 1) and ^{13}C-NMR (Table 2) spectra of **2** were superimposable on those of **1**, except for the signals due to an additional 3-hydroxyisobutyryl ester moiety [δ 1.03 (3H, d, J=7.0 Hz, 3HIB-4-H$_3$), 2.50 (1H, ddq, J=6.1, 6.1, 7.0 Hz, 3HIB-2-H), 3.42, 3.50 (1H each, both dd, J=6.1, 13.4 Hz, 3HIB-3-H$_2$)]. In the HMBC experiment of **2**, long-range correlations were observed between the 7-O-Rha-2-proton [δ 5.36 (1H, br s)] and the (2S)-2-methybutyryl ester carbonyl carbon (δ_C 174.8) and between the 7-O-terminal-Glc-6-protons [δ 3.87 (1H, dd, J=5.8, 11.0 Hz), 4.47 (1H, dd, J=1.8, 11.0 Hz)] and the 3-hydroxyisobutyryl ester carbonyl carbon (δ_C 174.1). Thus, sinocrassoside B$_5$ was elucidated as

quercetin 3-O-β-D-glucopyranosyl-7-O-β-D-(6-O-3-hydroxyisobutyryl)-glucopyranosyl-(1→3)-α-L-[2-O-(2S)-2-methylbutyryl]-rhamnopyranoside (**2**).

Sinocrassoside C$_1$ (**3**) was isolated as a yellow powder with negative optical rotation ([α]$_D^{25}$ −16.0° in MeOH). In the positive- and negative-ion FAB-MS of **3**, the quasimolecular ion peaks were observed at m/z 633 (M+Na)$^+$ and m/z 609 (M−H)$^-$, and the molecular formula C$_{27}$H$_{30}$O$_{16}$ was determined by high resolution FAB-MS measurement. Acid hydrolysis of **3** with 1.0 M HCl liberated herbacetin[18] (**35**) together with L-rhamnose and D-glucose, which were identified by HPLC analysis. The ^{1}H- (DMSO-d_6, Table 1) and ^{13}C-NMR (Table 2) spectra of **3** showed signals assignable to herbacetin (**35**) part [δ 6.61 (1H, s, H-6), 6.91, 8.13 (2H each, both d, J=8.9 Hz, 3′,5′,2′,6′-H)] together with a β-D-glucopyranosyl and a α-L-rhamnopyranosyl moieties [δ 1.12 (3H, d, J=6.1 Hz, Rha-6-H$_3$), 5.47 (1H, d, J=7.3 Hz, Glc-1-H), 5.50 (1H, br s, Rha-1-H)]. Finally, the connectivities of the β-D-glucopyranosyl and the α-L-rhamnopyranosyl moieties in **3** were elucidated on the basis of HMBC experiment, which showed long-range correlations were observed be-

Table 1. ^{1}H-NMR (500 MHz) Data of **1**—**6** and Related Compound (**1a**)

Position	**1** δ_H (J Hz)	**1a** δ_H (J Hz)	**2** δ_H (J Hz)	**3** δ_H (J Hz)	**4** δ_H (J Hz)	**5** δ_H (J Hz)	**6** δ_H (J Hz)
6	6.52 (d, 1.8)	6.47 (d, 1.8)	6.48 (d, 1.9)	6.61 (s)	6.60 (s)	6.62 (s)	6.59 (s)
8	6.89 (d, 1.8)	6.83 (d, 1.8)	6.87 (d, 1.9)				
2′	7.63 (d, 2.1)	7.63 (d, 2.1)	7.64 (d, 1.9)	8.13 (d, 8.9)	7.63 (d, 2.1)	7.68 (d, 2.1)	7.64 (d, 2.1)
3′				6.91 (d, 8.9)			
5′	6.86 (d, 8.2)	6.85 (d, 8.2)	6.85 (d, 8.3)	6.91 (d, 8.9)	6.86 (d, 8.2)	6.88 (d, 9.2)	6.85 (d, 9.2)
6′	7.62 (dd, 2.1, 8.2)	7.62 (dd, 2.1, 8.2)	7.62 (dd, 1.9, 8.3)	8.13 (d, 8.9)	7.62 (dd, 2.1, 8.2)	7.67 (dd, 2.1, 9.2)	7.63 (dd, 2.1, 9.2)
5-OH	12.61 (br s)	12.63 (br s)	12.61 (br s)	12.03 (br s)	11.90 (br s)	12.06 (br s)	12.06 (br s)
	(3-O-Glc)	(3-O-Glc)	(3-O-Glc)	(3-O-Glc)		(3-O-Glc)	(3-O-Glc)
1	5.49 (d, 7.0)	5.49 (d, 7.3)	5.49 (d, 7.0)	5.47 (d, 7.3)		5.48 (d, 7.6)	5.54 (d, 7.9)
2	3.26 (dd, 7.0, 8.5)	3.26 (dd, 7.3, 8.5)	3.26 (dd, 7.0, 8.5)	3.19 (dd, 7.3, 9.2)		3.28 (dd, 7.6, 9.2)	4.79 (dd, 7.9, 9.2)
3	3.22 (dd, 8.5, 9.2)	3.22 (dd, 8.5, 9.2)	3.19 (dd, 8.5, 9.2)	3.22 (dd, 9.2, 9.5)		3.25 (dd, 9.2, 9.5)	3.43 (dd, 9.2, 9.2)
4	3.09 (m)	3.10 (m)	3.09 (m)	3.09 (m)		3.10 (m)	3.17 (m)
5	3.10 (m)	3.11 (m)	3.10 (m)	3.09 (m)		3.12 (m)	3.21 (m)
6	3.33 (dd, 5.5, 11.2)	3.34 (dd, 5.5, 11.6)	3.33 (dd, 5.8, 11.0)	3.34 (dd, 5.8, 11.9)		3.34 (dd, 5.5, 11.0)	3.38 (dd, 5.8, 11.5)
	3.58 (dd, 1.8, 11.2)	3.58 (dd, 1.8, 11.6)	3.60 (dd, 1.8, 11.0)	3.56 (dd, 2.5, 11.9)		3.58 (dd, 2.1, 11.0)	3.60 (dd, 2.2, 11.5)
	(7-O-Rha)	(7-O-Rha)	(7-O-Rha)	(7-O-Rha)	(7-O-Rha)	(7-O-Rha)	(7-O-Rha)
1	5.70 (br s)	5.59 (br s)	5.70 (br s)	5.50 (br s)	5.51 (br s)	5.50 (d, 1.8)	5.47 (br s)
2	5.36 (br s)	4.11 (br s)	5.36 (br s)	3.95 (br s)	4.15 (br d, ca. 3)	3.97 (dd, 1.8, 3.0)	3.96 (br s)
3	4.00 (dd, 3.4, 9.5)	3.78 (dd, 3.4, 9.5)	3.96 (dd, 3.4, 9.5)	3.83 (dd, 2.8, 9.5)	5.11 (dd, 3.4, 9.8)	3.85 (dd, 3.0, 9.0)	3.83 (dd, 3.4, 9.2)
4	3.50 (dd, 9.5, 9.5)	3.52 (dd, 9.5, 9.5)	3.48 (dd, 9.5, 9.5)	3.32 (dd, 8.9, 9.5)	3.58 (dd, 9.5, 9.8)	3.34 (dd, 9.0, 9.5)	3.32 (dd, 9.2, 9.2)
5	3.60 (dq, 9.5, 5.8)	3.64 (dq, 9.5, 5.6)	3.59 (dq, 9.5, 5.8)	3.52 (dq, 8.9, 6.1)	3.76 (dq, 9.5, 6.1)	3.55 (dq, 9.5, 6.1)	3.54 (dq, 9.2, 6.1)
6	1.18 (d, 5.8)	1.14 (d, 5.6)	1.17 (d, 5.8)	1.12 (d, 6.1)	1.16 (d, 6.1)	1.14 (d, 6.1)	1.13 (d, 9.1)
	(7-O-Rha^3–^{1}Glc)	(7-O-Rha^3–^{1}Glc)	(7-O-Rha^3–^{1}Glc)				
1	4.47 (d, 7.6)	4.48 (d, 7.6)	4.47 (d, 7.7)				
2	3.00 (dd, 7.6, 9.5)	3.11 (dd, 7.6, 9.5)	3.02 (dd, 7.7, 9.5)				
3	3.18 (dd, 8.9, 9.5)	3.17 (dd, 8.9, 9.5)	3.21 (dd, 8.9, 9.5)				
4	3.01 (dd, 8.9, 9.5)	3.10 (dd, 8.9, 9.5)	3.04 (dd, 8.9, 9.5)				
5	3.19 (m)	3.19 (m)	3.42 (m)				
6	3.41 (dd, 5.8, 11.0)	3.47 (dd, 5.8, 11.5)	3.87 (dd, 5.8, 11.0)				
	3.67 (dd, 2.0, 11.0)	3.69 (dd, 1.9, 11.5)	4.47 (dd, 1.8, 11.0)				
acyl							
2	2.45 (ddq, 7.0, 7.0, 7.0)		2.41 (ddq, 7.0, 7.0, 6.7)		2.44 (ddq, 7.0, 7.0, 7.0)	2.03 (s)	
3	1.50 (ddq, 7.0, 14.0, 7.4)		1.50 (ddq, 7.0, 13.7, 7.4)		1.48 (ddq, 7.3, 15.0, 7.0)		
	1.64 (ddq, 7.0, 14.0, 7.4)		1.61 (ddq, 7.0, 13.7, 7.4)		1.64 (ddq, 7.3, 15.0, 7.0)		
4	0.93 (dd, 7.4, 7.4)		0.91 (dd, 7.4, 7.4)		0.90 (dd, 7.3, 7.3)		
5	1.12 (d, 7.0)		1.09 (d, 6.7)		1.12 (d, 7.0)		
2			2.50 (ddq, 6.1, 6.1, 7.0)				
3			3.42 (dd, 6.1, 13.4)				
			3.50 (dd, 6.1, 13.4)				
4			1.03 (d, 7.0)				

Measured in DMSO-d_6.

Table 2. ^{13}C-NMR (125 MHz) Data of **1**—**6** and Related Compound (**1a**)

Position	1 δ_C	1a δ_C	2 δ_C	3 δ_C	4 δ_C	5 δ_C	6 δ_C
2	156.7	156.6	156.8	156.6	147.8	156.7	156.9
3	133.6	133.5	133.7	133.1	135.8	133.2	132.8
4	177.5	177.5	177.6	177.8	176.2	177.8	177.5
5	160.8	160.8	160.8	152.0	151.6	152.0	152.0
6	99.3	99.4	99.5	98.7	98.8	98.6	98.7
7	161.2	161.2	160.8	150.4	150.0	150.4	150.6
8	94.4	94.4	94.5	127.0	127.3	127.0	127.1
9	155.8	155.8	155.8	144.4	144.8	144.4	144.5
10	105.7	105.6	105.9	105.4	104.8	105.4	105.4
1'	120.9	120.9	120.9	120.9	122.0	121.2	120.8
2'	116.3	116.2	116.3	131.0	115.4	116.5	116.4
3'	144.8	144.8	144.8	115.0	144.9	144.7	144.9
4'	148.6	148.6	148.7	160.0	147.5	148.5	148.9
5'	115.1	115.1	115.2	115.0	115.4	115.0	115.1
6'	121.6	121.6	121.7	131.0	120.3	121.8	122.0
	(3-O-Glc)	(3-O-Glc)	(3-O-Glc)	(3-O-Glc)		(3-O-Glc)	(3-O-Glc)
1	100.6	100.6	100.8	100.7		100.7	98.5
20	74.0	74.0	74.0	74.1		74.0	74.2
3	76.4	76.4	76.5	76.3		76.4	74.0
4	69.9	69.8	69.9	69.8		69.8	70.0
5	77.5	77.5	77.4	77.4		77.4	77.5
6	60.9	60.9	60.9	60.7		60.9	60.7
	(7-O-Rha)	(7-O-Rha)	(7-O-Rha)	(7-O-Rha)	(7-O-Rha)	(7-O-Rha)	(7-O-Rha)
1	94.7	98.2	94.9	99.3	99.4	99.3	99.5
2	70.5	68.9	70.8	69.8	67.4	69.8	69.8
3	77.8	80.6	78.2	69.9	73.1	69.9	69.9
4	70.6	70.4	70.5	71.6	68.8	71.7	71.7
5	69.3	69.5	69.3	69.8	69.9	69.8	69.8
6	17.8	17.8	17.8	17.8	17.7	17.8	17.8
	(7-O-Rha^3–^{1}Glc)	(7-O-Rha^3–^{1}Glc)	(7-O-Rha^3–^{1}Glc)				
1	104.3	104.5	104.4				
2	73.9	73.9	73.8				
3	76.0	76.1	75.9				
4	70.1	69.8	70.1				
5	76.5	76.7	74.0				
6	61.4	60.9	63.6				
acyl							
1	175.3		174.8		175.6		169.3
2	40.1		40.1		40.2		20.9
3	26.2		26.2		26.2		
4	11.1		11.0		11.2		
5	16.1		16.0		16.3		
1			174.1				
2			42.1				
3			63.1				
4			13.2				

Measured in DMSO-d_6.

tween the Glc-1-proton and the 3-carbon (δ_C 133.1) and between the Rha-1-proton and the 7-carbon (δ_C 150.4). Consequently, the structure of **3** was constructed as herbacetin 3-O-β-D-glucopyranosyl-7-O-α-L-rhamnopyranoside (**3**).

Sinocrassoside D$_1$ (**4**) was also isolated as a yellow powder with positive optical rotation ($[\alpha]_D^{23}$ +60.2° in MeOH). The UV and IR spectra of **4** indicated the flavonoid glycoside structure and the molecular formula, $C_{26}H_{28}O_{13}$, was determined by the quasimolecular ion peaks in positive- and negative-ion FAB-MS and by high resolution FAB-MS. Alkaline hydrolysis of **4** with 10% KOH–50% aqueous 1,4-dioxane (1:1, v/v) furnished gossypetin 7-O-α-L-rhamnopyranoside (**36**)[19,20] together with S-(+)-2-methylbutyric acid, which was identified by HPLC analysis using an optical rotation detector. The ^{1}H- (DMSO-d_6, Table 1) and ^{13}C-NMR (Table 2) spectra of **4** showed signals assignable to gossypetin (**37**)

part [δ 6.60 (1H, s, 6-H), 6.86 (1H, d, J=8.2 Hz, 5'-H), 7.62 (1H, dd, J=2.1, 8.2 Hz, 6'-H), 7.63 (1H, d, J=2.1 Hz, 2'-H)] and an α-L-rhamnopyranosyl moiety [δ 1.16 (3H, d, J=6.1 Hz, Rha-6-H$_3$), 5.51 (1H, br s, Rha-1-H)] together with (2S)-2-methylbutyryl moiety [δ 0.90 (3H, dd, J=7.3, 7.3 Hz, 2MB-4-H$_3$), 1.12 (3H, d, J=7.0 Hz, 2MB-5-H$_3$), 1.48, 1.64 (1H each, both ddq, J=7.3, 15.0, 7.0 Hz, 2MB-3-H$_2$), 2.44 (1H, ddq, J=7.0, 7.0, 7.0 Hz, 2MB-2-H)]. Finally, the position of (2S)-2-methylbutyryl group in **4** was confirmed by the HMBC experiment, which showed a long-range correlation between the Rha-3-proton [δ 5.11 (1H, dd, J=3.4, 9.8 Hz)] and the (2S)-2-methylbutyryl ester carbonyl carbon (δ_C 175.6). Consequently, the structure of sinocrassoside D$_1$ was determined as gossypetin 7-O-α-L-[3-O-(2S)-2-methylbutyryl]-rhamnopyranoside (**4**).

Sinocrassosides D$_2$ (**5**) and D$_3$ (**6**) were also isolated as a

white powder with positive optical rotation (5: $[\alpha]_D^{25}$ +71.3°, 6: $[\alpha]_D^{25}$ +150.6° both in MeOH), respectively. In the positive- and negative-ion FAB-MS of 5, the quasimolecular ion peaks were observed at m/z 649 $(M+Na)^+$ and m/z 625 $(M-H)^-$, and the molecular formula $C_{27}H_{30}O_{17}$ was determined by high-resolution FAB-MS measurement. The acid hydrolysis of 5 liberated gossypetin[18] (37) together with L-rhamnose and D-glucose. The proton and carbon signals in the ^{1}H- (DMSO-d_6, Table 1) and ^{13}C-NMR (Table 2) spectra of 5 showed signals due to a gossypetin moiety [δ 6.62 (1H, s, 6-H), 6.88 (1H, d, $J=9.2$ Hz, 5′-H), 7.67 (1H, dd, $J=2.1$, 9.2 Hz, 6′-H), 7.68 (1H, d, $J=2.1$ Hz, 2′-H)] together with a β-D-glucopyranosyl and a α-L-rhamnopyranosyl moieties [δ 1.14 (3H, d, $J=6.1$ Hz, Rha-6-H$_3$), 5.48 (1H, d, $J=7.6$ Hz, Glc-1-H), 5.50 (1H, d, $J=1.8$ Hz, Rha-1-H)]. The connectivities of the β-D-glucopyranosyl and α-L-rhamnopyranosyl moieties in 5 were clarified by HMBC experiment, in which long-range correlations were observed between the Glc-1-proton and the 3-carbon (δ_C 133.2) and between the Rha-1-proton and the 7-carbon (δ_C 150.4). Thus, the structure of sinocrassoside D$_2$ was determined as gossypetin 3-O-β-D-glucopyranosyl-7-O-α-L-rhamnopyranoside (5). On the other hand, the molecular formula, $C_{29}H_{32}O_{18}$, of 6 was determined by high resolution FAB-MS. Alkaline hydrolysis of 6 with 10% KOH–50% aqueous 1,4-dioxane (1 : 1, v/v) furnished 5 together with acetic acid, which was identified by HPLC analysis of its p-nitrobenzyl derivative. In the HMBC experiment of 6, a long-range correlation was observed between

the Glc-2-proton [δ 4.79 (1H, dd, $J=7.9$, 9.2 Hz)] and the acetyl carbonyl carbon (δ_C 169.3). On the basis of this evidence, the structure of sinocrassoside D$_3$ was determined as gossypetin 3-O-β-D-(2-O-acetyl)-glucopyranosyl-7-O-α-L-rhamnopyranoside (6).

Inhibitory Effects on Aminopeptidase N Activity Aminopeptidase N (APN) is a Zn$^+$-dependent metalloprotease and plays an important role in tumor-cell invasion, extracellular matrix degradation by tumor cells and tumor metastasis.[21,22] Recently, APN was identified on the endothelial cell surface as a receptor for a tumor-homing peptide motif, NGR (asparagines-glycine-arginine, Asn-Gly-Arg), which is capable of homing selectively to the tumor vasculature.[23] This evidence indicated that APN plays a critical role in angiogenesis. Accordingly, APN is considered as an important therapeutic target for tumor angiogenesis and metastasis. Previously, we have reported the isolation and structure elucidation of several flavonoids with APN inhibitory activity from the rhizomes of *Boesenbergia rotunda*.[24] As shown in Table 3, most of them except for megastigmane constituents (33, 34) were found to inhibit APN activity.[3] These activities were equivalent for that of curcumin (31.9±1.6% at 30 μM), which is known to show APN inhibitory activity.[25]

Inhibitory Effects on Rat Lens Aldose Reductase As a key enzyme in the polyol pathway, aldose reductase has been reported to catalyze the reduction of glucose to sorbitol. Sorbitol does not readily diffuse across cell membranes, and the intracellular accumulation of sorbitol has been implicated in

Table 3. Inhibitory Effects of Constituents from *S. indica* on Aminopeptidase N Activity

	Inhibition (%)		
	0 μM	10 μM	30 μM
Sinocrassoside B$_4$ (1)	0.0±0.9	12.0±1.0**	32.1±1.2**
Sinocrassoside B$_5$ (2)	0.0±1.2	20.9±1.2**	28.3±1.3**
Sinocrassoside C$_1$ (3)	0.0±1.2	5.6±1.1	12.4±1.3**
Sinocrassoside D$_1$ (4)	0.0±1.2	25.6±3.8**	35.1±0.9**
Sinocrassoside D$_3$ (6)	0.0±2.0	11.9±1.1**	23.2±0.8**
Sinocrassoside A$_1$ (7)	0.0±2.0	37.2±0.8**	31.4±0.2**
Sinocrassoside A$_2$ (8)	0.0±2.0	32.6±0.9**	35.7±0.4**
Sinocrassoside A$_4$ (10)[3]	0.0±2.0	26.8±0.6**	26.9±1.0**
Sinocrassoside A$_5$ (11)[3]	0.0±0.9	15.7±1.0**	21.7±0.5**
Sinocrassoside A$_6$ (12)[3]	0.0±0.9	12.4±0.7**	16.4±1.0**
Sinocrassoside A$_7$ (13)[3]	0.0±0.9	11.3±0.3**	23.7±0.8**
Sinocrassoside A$_9$ (15)	0.0±0.9	7.7±0.5*	19.9±0.6**
Sinocrassoside A$_{10}$ (16)	0.0±1.2	33.3±1.1**	28.7±1.1**
Sinocrassoside B$_1$ (19)	0.0±0.9	27.5±3.7**	33.9±1.0**
Sinocrassoside B$_2$ (20)	0.0±0.9	37.4±1.7**	39.4±0.4**
Sinocrassoside B$_3$ (21)[3]	0.0±0.9	22.7±1.0**	36.2±0.4**
Kaempferol (22)	0.0±0.4	6.8±1.3*	13.7±0.5**
Kaempferol 3-O-Glc (23)	0.0±0.4	7.1±1.8**	31.7±0.7**
Kaempferol 7-O-Rha (24)	0.0±0.4	6.2±0.8*	12.5±1.4**
Kaempferol 3-O-Glc 7-O-Rha (25)	0.0±0.4	6.9±2.7*	19.1±1.4**
Multiflorin B (26)	0.0±1.7	16.3±2.7*	32.8±1.4**
Kaempferol 3-O-Rha-(1→4)-Glc 7-O-Rha (27)	0.0±1.2	10.1±2.9**	13.8±0.6**
Quercetin (28)	0.0±1.7	6.2±1.6	18.1±3.0**
Quercetin 3-O-Glc (29)	0.0±1.7	12.6±8.2	41.8±0.9**
Quercetin 3-O-Glc 7-O-Rha (30)	0.0±1.7	4.4±2.3	12.6±1.1
Multinoside A (31)	0.0±1.2	−0.8±1.9	15.3±1.2**
Luteolin (32)	0.0±0.3	19.2±1.2**	60.2±1.7**
trans-(3S,5R,6R,9S)-Megastigman-7-ene-3,5,6,9-tetraol 3-O-Glc (33)	0.0±1.2	−2.9±1.9	−0.8±3.6
trans-(3S,5R,6R,9S)-Megastigman-7-ene-3,5,6,9-tetraol 9-O-Glc (34)	0.0±1.2	−1.0±0.8	−1.1±2.1
Curcumin[3]	0.0±1.7	13.3±0.9**	31.9±1.6**

Each value represents the mean±S.E.M. (n=4). Significantly different from the control, * $p<0.05$, ** $p<0.01$.

the chronic complications of diabetes such as cataract. Previously, we reported that various flavonoid and terpenoid constituents from several natural medicines and medicinal foods inhibited aldose reductase inhibitory activity.[4,26—31)] Since several flavonoid constituents were isolated from the whole plants of *S. indica*, the inhibitory effects of the principal flavonoid constituents on rat lens aldose reductase were examined. Among the flavonoid constituents from *S. indica*, kaempferol (**22**, $IC_{50}=10\,\mu$M), quercetin (**28**, $2.2\,\mu$M), quercetin 3-*O*-β-D-glucopyranoside (**29**, $4.5\,\mu$M), and luteolin (**32**, $0.45\,\mu$M), showed strong activity in agreement with the previous study.[4,28)] Additionally, sinocrassosides D_2 (**5**, $IC_{50}=47\,\mu$M) and A_2 (**8**, $31\,\mu$MM), multiflorin B (**26**, $2.7\,\mu$M), and quercetin 3-*O*-β-D-glucopyranosyl-7-*O*-α-L-rhamnopyranoside (**30**, $56\,\mu$M) were found to inhibit rat lens aldose reductase.

Experimental

The following instruments were used to obtain physical data: specific rotations, Horiba SEPA-300 digital polarimeter ($l=5$ cm); UV spectra, Shimadzu UV-1600 spectrometer; IR spectra, Shimadzu FTIR-8100 spectrometer; EI-MS and high-resolution MS, JEOL JMS-GCMATE mass spectrometer; FAB-MS and high-resolution MS, JEOL JMS-SX 102A mass spectrometer; ^{1}H-NMR spectra, JEOL EX-270 (270 MHz) and JNM-LA500 (500 MHz) spectrometers; ^{13}C-NMR spectra, JEOL EX-270 (68 MHz) and JNM-LA500 (125 MHz) spectrometers with tetramethylsilane as an internal standard; and HPLC detector, Shimadzu RID-6A refractive index and SPD-10A*vp* UV–VIS detectors. HPLC column, Cosmosil 5C_{18}-MS-II (Nacalai Tesque Inc., 250×4.6 mm i.d.) and (250×20 mm i.d.) columns were used for analytical and preparative purposes, respectively.

The following experimental conditions were used for chromatography: ordinary-phase silica gel column chromatography, Silica gel BW-200 (Fuji Silysia Chemical, Ltd., Aichi, Japan, 150—350 mesh); reversed-phase silica gel column chromatography, Chromatorex ODS DM1020T (Fuji Silysia Chemical, Ltd., Aichi, Japan, 100—200 mesh); TLC, precoated TLC plates with Silica gel 60F_{254} (Merck, 0.25 mm) (ordinary phase) and Silica gel RP-18 F_{254S} (Merck, 0.25 mm) (reversed phase); reversed-phase HPTLC, precoated TLC plates with Silica gel RP-18 WF_{254S} (Merck, 0.25 mm); and detection was achieved by spraying with 1% $Ce(SO_4)_2$–10% aqueous H_2SO_4 followed by heating.

Plant Material The whole plants of *S. indicum* cultivated at Guangxi province in China were purchased *via* Tochimoto Tenkaido Co., Ltd., Osaka, Japan. The plant material was identified by one of authors (T. W.). A voucher specimen (2004.02. Guangxi-02) of this plant is on file in our laboratory.[2)]

Extraction and Isolation Fraction 5-2 (770 mg) obtained from the EtOAc-soluble fraction and fractions 4-8 (970 mg), 5-5 (1980 mg), 5-6 (1030 mg), and 5-8 (1310 mg) from the *n*-BuOH-soluble fraction of the methanolic extract from the whole plant of *S. indica* (9.9 kg, cultivated in Guangxi province, China) as reported previously.[2)]

Fraction 5-2 (770 mg) from the EtOAc-soluble fraction was purified by HPLC [MeOH–H_2O (55 : 45, v/v)] to give sinocrassoside D_1 (**4**, 12.1 mg, 0.0006%) together with sinocrassosides A_7 (**13**, 23.0 mg, 0.0011%) and B_1 (**19**, 17.6 mg, 0.0009%) and quercetin (**28**, 96.6 mg, 0.0046%). Fraction 4-8 (970 mg) from the *n*-BuOH-soluble fraction was further purified by HPLC [MeOH–H_2O (55 : 45, v/v)] to give sinocrassosides B_4 (**1**, 348.6 mg, 0.0068%) and B_5 (**2**, 35.4 mg, 0.0007%) together with sinocrassosides A_8 (**14**, 72.0 mg, 0.0014%) and A_9 (**15**, 150.4 mg, 0.0029%). Fraction 5-5 (265 mg) from the *n*-BuOH-soluble fraction was subjected to HPLC [MeOH–H_2O (35 : 65, v/v)] to give sinocrassoside D_2 (**5**, 50.6 mg, 0.0074%). Fraction 5-6 (160 mg) from the *n*-BuOH-soluble fraction was subjected to HPLC [MeOH–H_2O (40 : 60, v/v)] to give sinocrassoside C_1 (**3**, 23.0 mg, 0.0027%) together with quercetin 3-*O*-β-D-glucopyranosyl-7-*O*-α-L-rhamnopyranoside (**30**, 14.7 mg, 0.0017%). Fraction 5-8 (300 mg) from the *n*-BuOH-soluble fraction was further purified by HPLC [MeOH–H_2O (40 : 60, v/v)] to give sinocrassoside D_3 (**6**, 11.5 mg, 0.0010%) together with sinocrassosides A_{11} (**17**, 15.8 mg, 0.0013%) and A_{12} (**18**, 13.1 mg, 0.0011%), kaempferol 3-*O*-β-D-glucopyranosyl-7-*O*-α-L-rhamnopyranoside (**25**, 17.9 mg, 0.0015%), quercetin 3-*O*-β-D-glucopyranosyl-7-*O*-α-L-rhamnopyranoside (**30**, 35.3 mg, 0.0030%), kaempferol 3-*O*-β-D-glucopyranosyl-(1→4)-α-L-rhamnopyranosyl-7-*O*-α-L-rhamnopyranoside (**27**, 9.6 mg,

0.0008%), and multinoside A (**31**, 27.6 mg, 0.0023%).

Sinocrassoside B_4 (**1**): A yellow powder, $[\alpha]_D^{25}$ −47.8° ($c=2.00$, MeOH). High-resolution positive-ion FAB-MS: Calcd for $C_{38}H_{48}O_{22}Na$ (M+Na)$^+$ 879.2535; Found 879.2540. UV [λ_{max} (log ε), MeOH]: 257 (4.49), 358 (4.37) nm. IR (KBr, cm^{-1}): 3432, 1725, 1655, 1599, 1076. ^{1}H-NMR (500 MHz, DMSO-d_6) δ: given in Table 1. ^{13}C-NMR (125 MHz, DMSO-d_6) δ_C: given in Table 2. Positive-ion FAB-MS *m/z*: 879 (M+Na)$^+$. Negative-ion FAB-MS *m/z*: 855 (M−H)$^-$.

Sinocrassoside B_5 (**2**): A yellow powder, $[\alpha]_D^{25}$ −64.5° ($c=2.00$, MeOH). High-resolution positive-ion FAB-MS: Calcd for $C_{42}H_{54}O_{24}Na$ (M+Na)$^+$ 965.2903; Found 965.2909. UV [λ_{max} (log ε), MeOH]: 257 (4.34), 357 (4.22) nm. IR (KBr, cm^{-1}): 3432, 1736, 1728, 1655, 1597, 1076. ^{1}H-NMR (500 MHz, DMSO-d_6) δ: given in Table 1. ^{13}C-NMR (125 MHz, DMSO-d_6) δ_C: given in Table 2. Positive-ion FAB-MS *m/z*: 965 (M+Na)$^+$. Negative-ion FAB-MS *m/z*: 941 (M−H)$^-$.

Sinocrassoside C_1 (**3**): A yellow powder, $[\alpha]_D^{25}$ −16.0° ($c=1.50$, MeOH). High-resolution positive-ion FAB-MS: Calcd for $C_{27}H_{30}O_{16}Na$ (M+Na)$^+$ 633.1432; Found 633.1425. UV [λ_{max} (log ε), MeOH]: 277 (4.28), 330 (4.11) nm. IR (KBr, cm^{-1}): 3432, 1655, 1603, 1057. ^{1}H-NMR (500 MHz, DMSO-d_6) δ: given in Table 1. ^{13}C-NMR (125 MHz, DMSO-d_6) δ_C: given in Table 2. Positive-ion FAB-MS *m/z*: 633 (M+Na)$^+$. Negative-ion FAB-MS *m/z*: 609 (M−H)$^-$.

Sinocrassoside D_1 (**4**): A yellow powder, $[\alpha]_D^{23}$ +60.2° ($c=0.80$, MeOH). High-resolution positive-ion FAB-MS: Calcd for $C_{26}H_{28}O_{13}Na$ (M+Na)$^+$ 571.1428; Found 571.1422. UV [λ_{max} (log ε), MeOH]: 261 (4.08), 344 (3.83) nm. IR (KBr, cm^{-1}): 3410, 1719, 1655, 1611, 1075. ^{1}H-NMR (500 MHz, DMSO-d_6) δ: given in Table 1. ^{13}C-NMR (125 MHz, DMSO-d_6) δ_C: given in Table 2. Positive-ion FAB-MS *m/z*: 571 (M+Na)$^+$. Negative-ion FAB-MS *m/z*: 547 (M−H)$^-$.

Sinocrassoside D_2 (**5**): A yellow powder, $[\alpha]_D^{25}$ +71.3° ($c=2.00$, MeOH). High-resolution positive-ion FAB-MS: Calcd for $C_{27}H_{30}O_{17}Na$ (M+Na)$^+$ 649.1381; Found 649.1385. UV [λ_{max} (log ε), MeOH]: 276 (4.26), 350 (4.08) nm. IR (KBr, cm^{-1}): 3410, 1655, 1605, 1059. ^{1}H-NMR (500 MHz, DMSO-d_6) δ: given in Table 1. ^{13}C-NMR (125 MHz, DMSO-d_6) δ_C: given in Table 2. Positive-ion FAB-MS *m/z*: 649 (M+Na)$^+$. Negative-ion FAB-MS *m/z*: 625 (M−H)$^-$.

Sinocrassoside D_3 (**6**): A yellow powder, $[\alpha]_D^{25}$ +150.6° ($c=0.70$, MeOH). High-resolution positive-ion FAB-MS: Calcd for $C_{29}H_{32}O_{18}Na$ (M+Na)$^+$ 691.1486; Found 691.1477. UV [λ_{max} (log ε), MeOH]: 259 (4.19), 349 (4.03) nm. IR (KBr, cm^{-1}): 3432, 1736, 1655, 1605, 1059. ^{1}H-NMR (500 MHz, DMSO-d_6) δ: given in Table 1. ^{13}C-NMR (125 MHz, DMSO-d_6) δ_C: given in Table 2. Positive-ion FAB-MS *m/z*: 691 (M+Na)$^+$. Negative-ion FAB-MS *m/z*: 667 (M−H)$^-$.

Alkaline Hydrolysis of 1, 2, 4, and 6 A solution of **1**, **2**, **4**, and **6** (each 5.0 mg) in 10% aqueous potassium hydroxide (KOH)–50% aqueous 1,4-dioxane (1 : 1, v/v, 1.0 ml) was stirred at 37 °C for 1 h. Removal of the solvent under reduced pressure gave a reaction mixture. A part of the reaction mixture was dissolved in dichloroethane (2.0 ml) and the solution was treated with *p*-nitrobenzyl-*N*-*N*′-diisopropylisourea (10 mg), then the whole was stirred at 80 °C for 1 h. The reaction solution was subjected to HPLC analysis [column: YMC-Pack ODS-A, 250×4.6 mm i.d.; mobile phase: MeOH (70 : 30, v/v); detection: UV (254 nm); flow rate: 0.9 ml/min] to identify the *p*-nitrobenzyl esters of acetic acid (**a**, t_R 6.2 min) from **6**, 3-hydroxyisobutyric acid (**b**, t_R 10.5 min) from **2**, and 2-methylbutyric acid (**c**, t_R 16.9 min) from **1**, **2**, and **4**, which were carried out by comparison of their retention time with those of commercially obtained standard samples. The rest of the reaction mixture was neutralized with Dowex HCR W2 (H$^+$ form) and the resin was removed by filtration. Evaporation of the solvent from the filtrate under reduced pressure yielded a product. A part of the product was subjected to HPLC analysis [column: YMC-Pack ODS-AQ, 250×4.6 mm i.d.; mobile phase: CH_3CN–0.1% aqueous H_3PO_4 (20 : 80, v/v); detection: optical rotation [Shodex OR-2 (Showa Denko Co., Ltd., Tokyo, Japan)]; flow rate: 1.0 ml/min] to identify S-(+)-2-methylbutyric acid [**c'**, t_R 15.4 min (positive)] from **1**, **2**, and **4**, which was carried out by comparison of its retention time and optical rotation with that of commercially obtained standard sample. The rest of the product was subjected to HPLC [MeOH–H_2O (50 : 50 v/v)] to give quercetin 3-*O*-β-D-glucopyranosyl-7-*O*-β-D-glucopyranosyl(1→3)-α-L-rhamnopyranoside (**1a**, 1.0 mg from **1**, 1.0 mg from **2**), gossypetin 7-*O*-α-L-rhamnopyranoside[19,20)] (**36**, 1.8 mg from **4**), and **5** (1.8 mg, from **6**).

Quercetin 3-*O*-β-D-Glucopyranosyl-7-*O*-β-D-glucopyranosyl-(1→3)-α-L-rhamnopyranoside (1a) A yellow powder, $[\alpha]_D^{23}$ −108.2° ($c=0.50$, MeOH). High-resolution positive-ion FAB-MS: Calcd for $C_{33}H_{40}O_{21}Na$ (M+Na)$^+$ 795.1960; Found 795.1967. UV [λ_{max} (log ε), MeOH]: 257

(4.40), 358 (4.37) nm. IR (KBr, cm^{-1}): 3432, 1655, 1599, 1076. ^{1}H-NMR (500 MHz, DMSO-d_6) δ: given in Table 1. ^{13}C-NMR (125 MHz, DMSO-d_6) δ_C: given in Table 2. Positive-ion FAB-MS m/z: 795 (M+Na)$^+$. Negative-ion FAB-MS m/z: 771 (M−H)$^-$.

Acid Hydrolysis of 3, 5, and 1a A solution of **3**, **5**, and **1a** (each 1.0 mg) in 1 M HCl (2.0 ml) was heated under reflux for 3 h. After cooling, the reaction mixture was extracted with EtOAc. The EtOAc-soluble fraction was subjected to HPLC analysis under the following conditions, respectively: HPLC column, YMC-Pack ODS-A, 4.6 mm i.d.×250 mm (YMC Co., Ltd., Ktoyo, Japan); detection, UV (254 nm); mobile phase, MeOH–1% aqueous AcOH (60:40, v/v); flow rate 1.0 ml/min]. Identification of gossypetin (**37**, from **5**), herbacetin (**35**, from **3**), and quercetin (**28**, from **1a**) present in the EtOAc-soluble fraction was carried out by comparison of their retention time with those of authentic samples (t_R: **37**, 5.0 min; **35**, 7.5 min; and **28**, 9.0 min). On the other hand, the aqueous layer was subjected to HPLC analysis under the following conditions, respectively: HPLC column, Kaseisorb LC NH$_2$-60-5, 4.6 mm i.d.×250 mm (Tokyo Kasei Co., Ltd., Tokyo, Japan); detection, optical rotation [Shodex OR-2 (Showa Denko Co., Ltd., Tokyo, Japan); mobile phase, CH$_3$CN–H$_2$O (85:15, v/v); flow rate 0.8 ml/min]. Identification of L-rhamnose (i) and D-glucose (ii) from **3**, **5**, and **1a** present in the aqueous layer was carried out by comparison of their retention time and optical rotation with those of an authentic samples [t_R: (i) 7.8 min (negative optical rotation) and (ii) 13.9 min (positive optical rotation)].

Bioassay Method. Effects on Aminopeptidase N Inhibitory Activity Aminopeptidase N activity was assayed by the method described in a previous report.[24] Briefly, 0.2 mM of the enzyme substrate, L-alanine-4-methylcoumaryl-7-amide (Ala-MCA, Peptide Institute) in 50 mM Tris–HCl buffer containing 200 mM NaCl (pH 8.0, 100 μl/well) and sample solution (20 μl) in 96-well black microplates. The reaction mixture was initiated by adding an enzyme solution 100 μl/well (rat, 1 μU, Calbiochem) and incubated at 37 °C for 1 h to convert Ala-MCA to a fluorescent product, 7-amino-4-methylcoumarin (AMC). The reaction mixture was mixed with 0.1 M EDTA (50 μl/well) to stop the reaction. Fluorescence was measured using a fluorescence microplate reader (FLUOstar OPTIMA, BMG Labtechnologies) at an excitation wavelength of 380 nm and an emission wavelength of 460 nm. Each sample was dissolved in dimethyl sulfoxide (DMSO) and diluted with PBS (final DMSO concentration in the incubation mixture was 0.1%). Curcumin was isolated from Thai Zedoary (the rhizomes of *Curcuma zedoaria* originating in Thailand)[32] and used as a reference compound.

Effects on Aldose Reductase Inhibitory Activity Aldose reductase activity was assayed by the method described previously.[4,26—31] The supernatant fluid of rat lens homogenate was used as a crude enzyme. The incubation mixture contained 135 mM Na, K-phosphate buffer (pH 7.0), 100 mM Li$_2$SO$_4$, 0.03 mM NADPH, 1 mM DL-glyceraldehyde as a substrate, and 100 μl of enzyme fraction, with or without 25 μl of sample solution, in a total volume of 0.5 ml. The reaction was initiated by the addition of NADPH at 30 °C. After 30 min, the reaction was stopped by the addition of 150 μl of 0.5 M HCl. Then, 0.5 ml 6 M NaOH containing 10 mM imidazole was added, and the solution was heated at 60 °C for 20 min to convert NADP to a fluorescent product. Fluorescence was measured using a fluorophotometer (Luminescence Spectrometer LS50B, Perkin Elmer, U.K.) at an excitation wavelength of 360 nm and an emission wavelength of 460 nm.

Statistics Values are expressed as means±S.E.M. One-way analysis of variance followed by Dunnett's test was used for statistical analysis.

References and Notes

1) Part XXXI: Ninomiya K., Morikawa T., Xie H., Matsuda H., Yoshikawa M., *Heterocycles*, **75**, 1983—1995 (2008).
2) Yoshikawa M., Wang T., Morikawa T., Xie H., Matsuda H., *Chem. Pharm. Bull.*, **55**, 1308—1315 (2007).
3) Morikawa T., Xie H., Wang T., Matsuda H., Yoshikawa M., *Chem. Biodiver.*, (2008), in press.
4) Xie H., Wang T., Matsuda H., Morikawa T., Yoshikawa M., Tani T., *Chem. Pharm. Bull.*, **53**, 1416—1422 (2005).
5) Morikawa T., Xie H., Matsuda H., Yoshikawa M., *J. Nat. Prod.*, **69**, 881—886 (2006).
6) Morikawa T., Xie H., Matsuda H., Wang T., Yoshikawa M., *Chem. Pharm. Bull.*, **54**, 506—513 (2006).
7) Xie H., Morikawa T., Matsuda H., Nakamura S., Muraoka O., Yoshikawa M., *Chem. Pharm. Bull.*, **54**, 669—675 (2006).
8) Yoshikawa M., Matsuda H., Morikawa T., Xie H., Nakamura S., Muraoka O., *Bioorg. Med. Chem.*, **14**, 7468—7475 (2006).
9) Matsuda H., Sugimoto S., Morikawa T., Matsuhira K., Mizuguchi E., Nakamura S., Yoshikawa M., *Chem. Pharm. Bull.*, **55**, 106—110 (2007).
10) Yoshikawa M., Morikawa T., Zhang Y., Nakamura S., Muraoka O., Matsuda H., *J. Nat. Prod.*, **70**, 575—583 (2007).
11) Morikawa T., Zhang Y., Nakamura S., Matsuda H., Muraoka O., Yoshikawa M., *Chem. Pharm. Bull.*, **55**, 435—441 (2007).
12) Ninomiya K., Morikawa T., Zhang Y., Nakamura S., Matsuda H., Muraoka O., Yoshikawa M., *Chem. Pharm. Bull.*, **55**, 1185—1191 (2007).
13) Zhang Y., Morikawa T., Nakamura S., Ninomiya K., Matsuda H., Muraoka O., Yoshikawa M., *Heterocycles*, **71**, 1565—1576 (2007).
14) Nakamura S., Li X., Matsuda H., Ninomiya K., Morikawa T., Yamaguti K., Yoshikawa M., *Chem. Pharm. Bull.*, **55**, 1505—1511 (2007).
15) Nakamura S., Li X., Matsuda H., Yoshikawa M., *Chem. Pharm. Bull.*, **56**, 536—540 (2008).
16) Li X., Nakamura S., Matsuda H., Yoshikawa M., *Chem. Pharm. Bull.*, **56**, 612—615 (2008).
17) Yoshikawa M., Nakamura S., Li X., Matsuda H., *Chem. Pharm. Bull.*, **56**, 695—700 (2008).
18) These standard samples were purchased from Apin Chemicals Ltd. (U.K.).
19) Zapesochnaya G. G., Kurkin V. A., Schavlinskii A. N., *Khim. Prir. Soedin.*, **1985**, 496—507 (1985).
20) Yoshikawa M., Shimada H., Shimoda H., Murakami N., Yamahara J., Matsauda H., *Chem. Pharm. Bull.*, **44**, 2086—2091 (1996).
21) Look A. T., Ashmum R. A., Shapiro L. H., Peiper S. C., *J. Clin. Invest.*, **83**, 1299—1307 (1989).
22) Saiki I., Fujii H., Yoneda J., Abe F., Nakajima M., Tsuruo T., Azuma I., *Int. J. Cancer*, **54**, 137—143 (1993).
23) Pasqualini R., Koivunen E., Kain R., Lahdenranta J., Sakamoto M. M., Stryhn A., Ashmum R. A., Shapiro L. H., Arap W., Ruoslahti E., *Cancer Res.*, **60**, 722—727 (2000).
24) Morikawa T., Funakoshi K., Ninomiya K., Yasuda D., Miyagawa K., Matsuda H., Yoshikawa M., *Chem. Pharm. Bull.*, **56**, 956—962 (2008).
25) Shim J. S., Kim J. H., Cho H. Y., Yum Y. N., Kim S. H., Park H.-J., Shim B. S., Choi S. H., Kwon H. J., *Chem. Biol.*, **10**, 695—704 (2003).
26) Yoshikawa M., Morikawa T., Murakami T., Toguchida I., Harima S., Matsuda H., *Chem. Pharm. Bull.*, **47**, 340—345 (1999).
27) Matsuda H., Morikawa T., Ueda H., Yoshikawa M., *Heterocycles*, **55**, 1499—1504 (2001).
28) Matsuda H., Morikawa T., Toguchida I., Yoshikawa M., *Chem. Pharm. Bull.*, **50**, 788—795 (2002).
29) Matsuda H., Morikawa T., Toguchida I., Harima S., Yoshikawa M., *Chem. Pharm. Bull.*, **50**, 972—975 (2002).
30) Yoshikawa M., Murakami T., Ishiwada T., Morikawa T., Kagawa M., Higashi Y., Matsuda H., *J. Nat. Prod.*, **65**, 1151—1155 (2002).
31) Morikawa T., Kishi A., Pongpiriyadacha Y., Matsuda H., Yoshikawa M., *J. Nat. Prod.*, **66**, 1191—1196 (2003).
32) Matsuda H., Tewtrakul S., Morikawa T., Nakamura A., Yoshikawa M., *Bioorg. Med. Chem.*, **12**, 5891—5898 (2004).